RIM Propeller for Micro Autonomous Underwater Vehicles

Citation: Kim, David Donghyun, You Wu, Antoine Noel, and Kamal Youcef-Toumi. "RIM Propeller for Micro Autonomous Underwater Vehicles." Volume 3: Industrial Applications; Modeling for Oil and Gas, Control and Validation, Estimation, and Control of Automotive Systems; Multi-Agent and Networked Systems; Control System Design; Physical Human-Robot Interaction; Rehabilitation Robotics; Sensing and Actuation for Control; Biomedical Systems; Time Delay Systems and Stability; Unmanned Ground and Surface Robotics; Vehicle Motion Controls; Vibration Analysis and Isolation; Vibration and Control for Energy Harvesting; Wind Energy (October 22, 2014).

As Published: http://dx.doi.org/10.1115/DSCC2014-6282

Publisher: ASME International

Persistent URL: http://hdl.handle.net/1721.1/120039

Version: Final published version: final published article, as it appeared in a journal, conference proceedings, or other formally published context

Proceedings of the ASME 2014 Dynamic Systems and Control Conference
DSCC2014
October 22-24, 2014, San Antonio, TX, USA

DSCC2014-6282

RIM PROPELLER FOR MICRO AUTONOMOUS UNDERWATER VEHICLES

David Donghyun Kim, You Wu, Antoine Noel, Kamal Youcef-Toumi*
Mechatronics Research Laboratory
Department of Mechanical Engineering
Massachesetts Institute of Technology
Cambridge, MA 02139
Email: youcef@mit.edu

ABSTRACT

Micro autonomous underwater vehicles (AUVs) need small-scale, powerful and safe propulsion systems especially when they are performing missions in pipes and other confined environments. However, the most conventional propulsion systems do not satisfy all three requirements: small, powerful and safe. A micro propulsion system meeting those requirements are developed based on the RIM propeller concept. It is compact and powerful; the complete motor-propeller assembly is 33mm in diameter, 12mm in depth and 16g in weight, and it is capable of producing 0.4N thrust in static water given a 7.1W power input. The paper presents the design, manufacturing and integration of the micro RIM propeller in an AUV.

INTRODUCTION

There has been a recent increase in robotic missions in confined environments. Robotic platforms are sent into 10 cm diameter gas and water pipe networks to detect leaks. [1] [2] [3] [4] [5] Autonomous Underwater Vehicles are used to inspect the interiors of nuclear reactors. [6] [7] [8] Operators send micro autonomous underwater vehicles AUVs into those confined environments to pinpoint the exact locations of the problems such as leaks and defects. In many cases, such problems cannot be sensed remotely.

There are four main challenges for AUVs to maneuver in confined environments. The challenges are the size constraint, high maneuverability requirement, harsh environment and safety concerns. They can be explained using as an example the pipe inspection robot being developed by researchers at the Mechatronics Research Laboratory (MRL) within Massachusetts Institute of Technology (MIT). It is designed for operating inside 10 cm (4 inch) pipes when 1 m/s water flow is present. It needs to make turns at certain T junctions to follow a desired path. The first challenge is the size constraint. In the confined environments such as the 10-15 cm diameter water pipes commonly used in many city water distribution networks, the space for the AUVs to move is very limited. There are often obstacles such as Calcium deposits in the pipe blocking the path of the AUVs such

FIGURE 1. MICRO RIM PROPELLER PRESENTED IN THIS PAPER

*Address all correspondence to this author.

that only AUVs smaller than certain size can fit through. The second challenge is about maneuverability. It takes fine control and fast response to make a sharp 90 degree turn at a T junction and zigzag through the maze of pipes. The third challenge is the harsh environment and in this case it is the strong turbulent flow. The drag force created by the 1 m/s flow in the pipe can make it impossible for some small AUVs brake or turn in the direction of the flow. The turbulence in the confined environment makes it even more difficult to perform maneuvers accurately. The last challenge is concerned with safety issues such as collision. AUVs can easily bump into the boundaries of the environment such as the pipe walls. If the robot loses its mobility or any other functionality due to collision, it may block or contaminate the water distribution system instead of fixing problems.

Those four challenges put a high bar on the sensing, control and actuation requirement on the AUVs, and this paper focus on the actuators. To overcome those challenges, an AUV requires a set of compact, powerful, safe and easy-to-integrate propulsion systems. The ideal propulsion systems must be compact and easy to integrate so they can be packaged into a micro AUV. They are the main actuator providing the thrust required for the vehicle to maneuver in turbulent flows. The propulsion system should not fail in the case of collision.

External propulsion systems are an important type of actuator for AUVs. External systems such as regular motor driven propellers are powerful but they are not safe. When colliding with walls, rigid propeller blades can easily get damaged and flexible blades will deform and lose their thrust outputs. Another type of external propulsion system is the biomimetic swimming mechanism used on soft robots [9] [10]. Although they are very safe against possible collisions, current micro biomimetic systems are slow comparing to systems with propellers.

Internal propulsion systems are the other important type actuator for AUVs and they have their pros and cons too. They are safe for operating in the confined environment. Internal propulsion systems such as micro pumps and duct propellers are contained and protected inside the vehicle, reducing the chance of damage due to collisions. Micro pumps are compact, safe and easy to integrate into the vehicle but generally not powerful. The TCS M400S is one of the most powerful pump for its size, $40\times26\times25$ mm. However, even with the optimal outlet size, it can only produce up to 0.25N thrust given a 7.1W power input [11]. Ducted propellers can provide a large thrust output, but their size and complexity can make it difficult to integrate them into a small robot. As shown in Fig. 2, the motor that drives the propellers and the watertight bearing take the valuable space out of the compact vehicle.

Compare to the conventional propulsion systems discussed above, the RIM driven propeller [12] [13] has more potential in satisfying all four requirements: being compact, powerful, safe and easy to integrate. RIM propeller is an internal propulsion system that is similar to ducted propeller, but its motor is placed

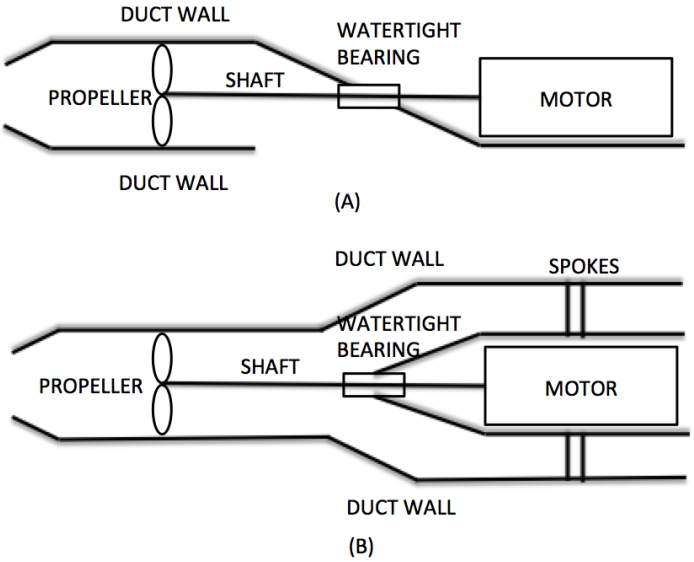

FIGURE 2. TWO COMMON CONFIGURATIONS OF DUCTED PROPELLERS. (A) WATER INLET ON THE SIDE (B) WATER INLET ALONG THE PROPELLER AXIS

differently. It is a propeller built into a DC brushless motor; the rotor portion of a DC brushless inrunner is hollowed out and replaced with the propeller blades. RIM driven propeller is a compact and integrated product that can be easily built into an AUV.

However, to the best of our knowledge, there has not been attempts to adopt RIM driven propellers in micro AUV applications yet. Most of the past and current development of RIM driven propellers are of large diameter, and the smallest one is 70 mm in diameter and consumes about more than 60W of electricity [13]. Micro RIM propellers which are as small as the TCS M400S micro pump and operates on a small pack of battery have not been seen in literatures yet. RIM propellers are safe because their shaft-less design prevents them from getting entangled with soft objects floating in the water [13] [14]. However, it is barely discussed in the literature how to suspend the propeller without a shaft in a micro scale structure. It is commonly known that, if the air gap between the stator and the rotor is not maintained uniform, the motor will suffer from the loss of efficiency. Due to the challenges in manufacturing and suspension, the RIM propeller for micro AUVs have not been proved in practice yet.

In this paper, we specifically present the design, manufacturing and performance analysis of a RIM propeller for micro AUVs as shown in Fig. 1. A few variations of the RIM propeller, including the stator material, the stator size and the bearing structure are compared. An example of the integration of the RIM propeller in an AUV is also described at the end of this

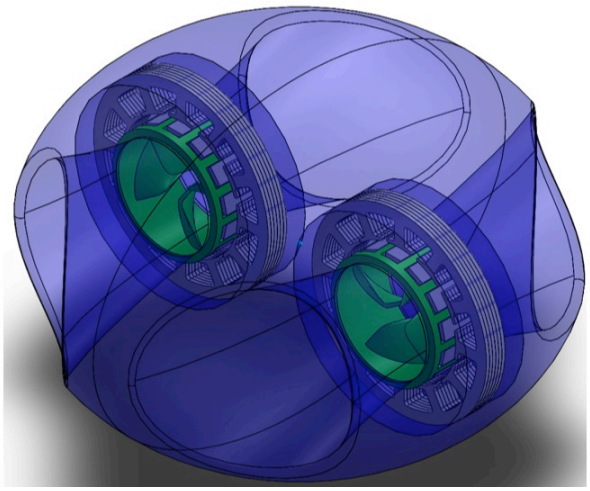

FIGURE 3. DESIGN OF THE AUV WITH A PAIRS OF RIM PROPELLERS

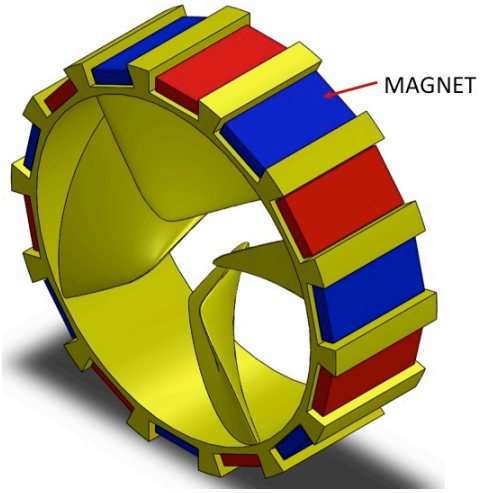

FIGURE 4. ISOMETRIC VIEW OF THE ROTOR

paper.

DESIGN AND MANUFACTURE

Design Requirements

This micro RIM propeller is designed to meet the performance requirement of the pipe inspection robot under development at MIT. Two RIM propellers are planned to be placed in the robot as shown in Fig 3. This robot has an ellipsoid shape, and its dimensions are 85 mm long, 85 mm wide and 60 mm high. It is designed to maneuver inside 100 mm diameter water pipelines. The target velocity of the vehicle with respect to the water stream is 1m/s. The CFD simulation with ANSYS Fluent CFD predicts the drag force on a perfect ellipsoid shape of this dimension inside the pipe is about 1.4N, while with the two ducts as shown in Fig. 3, it is reduced to 0.6N. In this robot, RIM propellers are used as ducted propellers. Putting a safety factor in place, we set (1) the thrust requirement to be 0.4N per propeller. The robot operates on a small pack of Lipo battery so (2) each propeller should consume no more than 10W of electric power. Based on the size constraint and the space layout of the robot, design specifications for each RIM propeller assembly are determined to be: (3) maximum 36mm in diameter, (4) maximum 15mm in depth (5) propeller portion must fit into a 19mm diameter duct.

Rotor

The rotor is designed based on the common brushless DC motor. Most of the conventional brushless DC motors are built with 3 phase electrical circuit that is connected to a common ground. The controller of the motor will connect two of the 3 phases and send a specified current. A common brushless dc inrunner motor is constructed such that the rotor containing the permanent magnet is attached to a shaft in the center, and the stator with the coil winding is place on the exterior circumference. When modifying its design to be a RIM propeller, the stator is unchanged, while the rotor is hollowed out and made into a ring shape. The propeller blades are then built inside the ring and the permanent magnets are attached outside of the ring, as indicated in Fig. 4. Slots are designed on the outer ring to hold the magnets in place.

The permanent magnets on the rotor are selected based on size and magnetic strength. Given the size constraint of the RIM propeller, each piece of the permanent magnets must be thin or curved so the circular shape of the rotor is maintained. NdFeB, Grade N42 block magnets of dimension 6.350mm $\times$ 3.175mm $\times$ 0.794mm (1/4in $\times$ 1/8in $\times$ 1/32in) are selected. The vendor is K&J Magnetics, Inc. The surface field strength is 2186 Gauss. The N42 grade NdFeB magnet is a commonly used rare earth material that is easily accessible. Having as many magnets as possible on the rotor will provide evenly distributed magnetic field strength along the circumference of the rotor. With the inner diameter of the rotor to be 19mm, the maximum number of magnets is found to be 14 as shown in Fig. 4. Common practice of motor design requires the number of poles of the magnets to be even number and different from the number of poles of the stator.

Propeller Blades

The propeller blades are designed based on Blade Element Theory. In the same ANSYS Fluent CFD simulation, the induced flow speed inside the duct is found to be 2 m/s. The maximum allowable dimension of the propeller is 19mm in diameter and 7mm in thickness, or it will not fit into the duct. 4000 rpm angular velocity and 0.4N target thrust. An optimized four blades propeller with elliptical sections is able to generate desired thrust

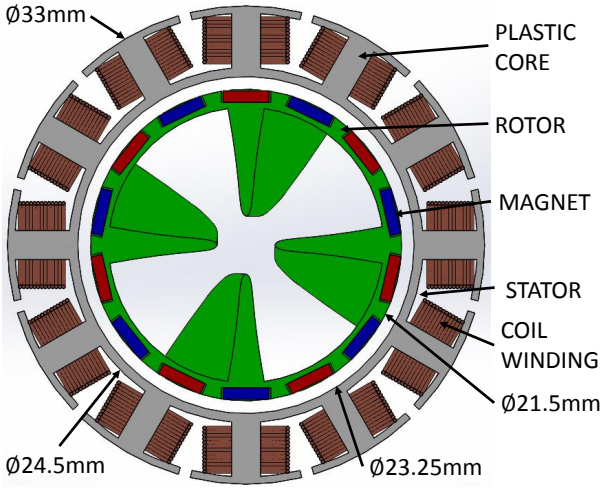

FIGURE 5. STATOR DESIGN WITH PLASTIC CORE MATERIAL

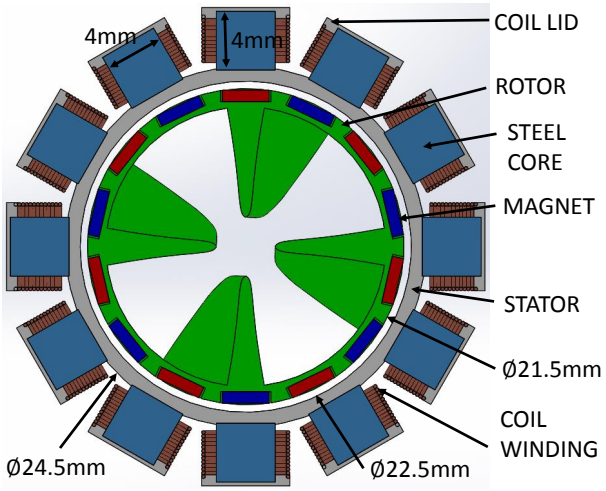

FIGURE 6. STATOR DESIGN WITH DISCONTINUOUS STEEL CORE

efficiently at target angular velocity. Further optimization with more advanced propeller design theories and CFD tools can be done to improve the performance of the propeller.

The rotor including the four blades and the exterior ring for holding the magnets are 3D printed as one piece. The 3D printer used here is the Stratasys Fortus 250mc FDM printer. It is configured to print ABS thermoplastic at a slice height of 0.178mm. The ring of the rotor is designed to be 1.5mm thick so the 3D printed part can be rigid. Since most of the parts in this micro RIM propeller are 3D printed, the same minimum thickness is applied to all of them. The magnets are then attached to the rotor with Loctite® 401 super glue. After the glue was applied, the rotor is wrapped with a thin Permacel® tape to further prevent the magnets from falling out of rotor assembly in the case of sudden changes in torques or impact. The Permacel® tape also makes the outer surface of the rotor smooth. The fully assembled rotor, including magnets, propeller and the tape, weights 1.7 grams.

Stator

Three designs of the stator were evaluated. Similar to that in a brushless DC motor, the stator consists of the stator cores and the coil windings. The stator core can be built with three different configurations as shown in Fig. 5 to Fig. 7. They are plastic core design, discontinuous steel core design and continuous steel core design.

The first design in Fig. 5 uses the 3D printed plastic as the core material with the openings on the outside. There are two benefits to this design. The stator poles can be accessed from outside, making it relatively easy to apply coil windings. Since the stator is made out of plastic, the weight of the motor assembly will be very light when compared to that made out of the other materials. However, the torque generation of the plastic stator is expected to be significantly lower because the permeability of the plastic is much lower than that of steel. 53 turns of Gauge 30 magnetic copper wires are wrapped around each stator pole. From theory of electro-magnets, larger the number of coil winding, the stronger induced magnetic field would be. The spacing between the poles allows 53 turns of coil winding as the maximum value.

The next two designs utilize the high permeability materials to concentrate the magnetic field and enhance the efficiency of the motor. Fig. 6 uses individual pieces of steel cylinders as the cores and have coils winding on them. It is the same dimension as the plastic stator in Fig. 5. This design was supposed to combine the light weight of the plastic material and the high permeability of steels for better performance to weight ratio. However, it turned out to be ineffective because the magnetic field will not circulate between the different stator poles to create torque effectively. In the experiment, the torque generated could not even overcome the attraction force between the steel cores and the permanent magnets. As a result, the rotor constantly vibrated back and forth instead of rotating continuously.

Fig. 7 shows the continuous steel stator design that is the closest to the stators in conventional motor. The steel core in the center of each winding concentrates the magnetic field in each coil while a steel outer ring helps the circulation of the magnetic field and conserves it. The detail of the magnetic field generation is discussed in the simulation and experimentation section. The stator cores are manufactured in 6 layers of gauge 24 non-oriented laminated steel. This construction reduces the formation of eddy currents. Each layer of the laminated steel is water-jetted. Although water-jet is accurate, the stator cores are made thicker than its plastic counterparts for rigidity issues. Since the cores are thicker, only 40 turns of the winding fit on each one of the 12 poles.

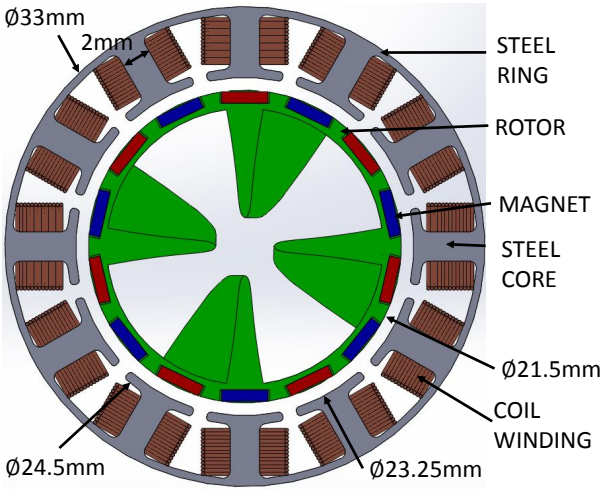

FIGURE 7. STATOR DESIGN WITH CONTINUOUS STEEL CORE

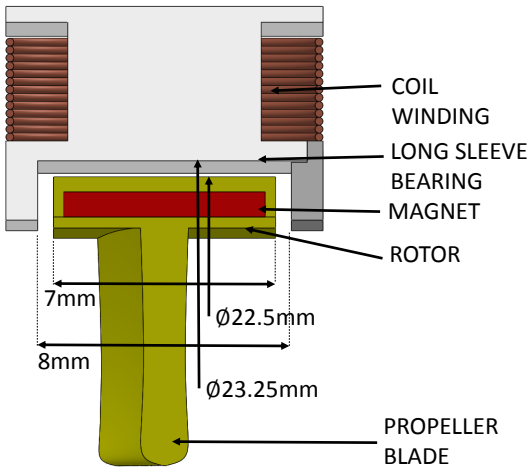

FIGURE 8. BEARING DESIGN OPTION 1, LONG SLEEVE BEARING, CROSS SECTION VIEW

For all the stator configurations, 12 poles are chosen based on the motor design fundamentals and experiments. The brushless DC motor will have 3 phase circuit which requires the number of coils to be a multiple of 3. Stators with 3, 6, 9 and 12 poles were attempted in manufacturing. The stator windings are applied manually. With 3, 6 or 9 poles, the distance between the closest two poles were too big to produce an even magnetic field around the circumference. 12 poles produced the most even magnetic field compared to the previous three. However, as the number of poles increased, the space between two poles reduced and it became increasingly difficult to apply coil windings on the poles. For manufacturability and performance, 12 poles were the optimal choice.

Bearing

The rotor suspension in RIM propellers is an important challenge. Bearings maintain the uniform air gap between the stator poles and rotor poles, allowing uniform and smooth torque generation. It also minimizes the friction loss during the operation. The common inrunner motor designs use ball bearing assembly. For this micro RIM propeller, putting in a ball bearing is going to increase the complexity and size. In order to install the bearing, the stator unit should have a shaft or another supporting structure to extrude in both sides of the propeller. It is not desired to increase the length or any dimension of the RIM propeller.

We considered two options for bearings, and the first one is a long sleeve bearing. It is built into the stator housing and placed between the stator poles and the rotor. The inner surface of the sleeve bearing is smooth, and it is in slide contact with the outer ring of the rotor. In order to reduce the mechanical friction, the rotor is slightly smaller than the bearing. The long sleeve bearing can be made out of Teflon or coated with Teflon to lower the

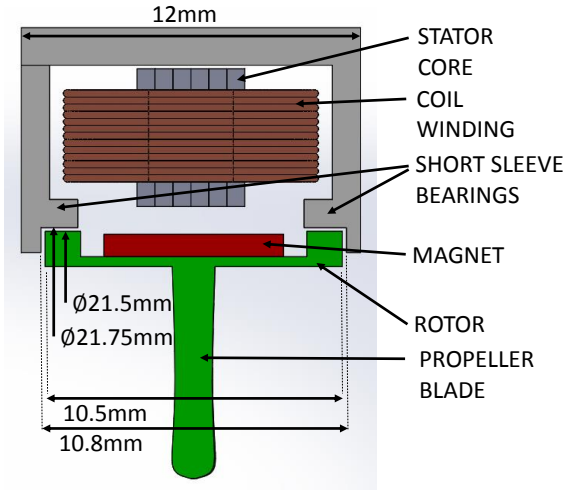

FIGURE 9. BEARING DESIGN OPTION 2, TWO SHORT SLEEVE BEARINGS, CROSS SECTION VIEW

friction. The section view of the long sleeve bearing is displayed in Fig. 8. With the long sleeve bearing, the stator housing covers the stator completely and prevent water from contacting the stator. The long sleeve bearing must be made thin in order to minimize the gap between the magnets and the coils. The size of this gap determines the efficiency of torque generation. In our practice, the whole stator housing was 3D printed and the inner surface of the bearing was applied with Teflon coating. The long sleeve bearing is 1.5mm thick considering the rigidity of 3D printed parts.

The second option for bearings we considered is a pair of short sleeve bearings. Like most conventional motors use two bearings one at each end of the shaft, two short sleeve bearings

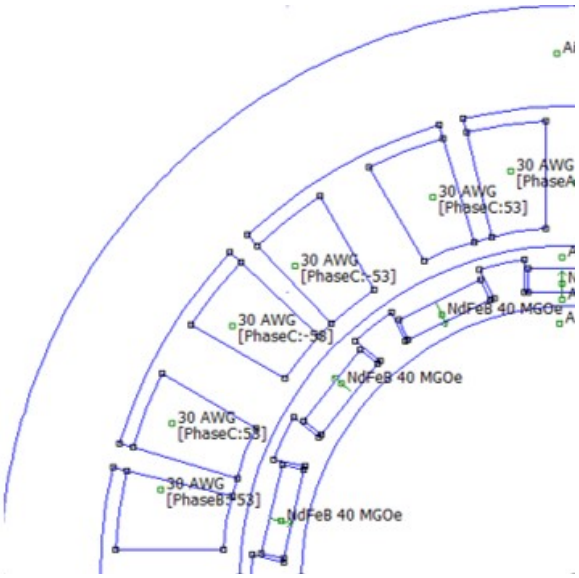

FIGURE 10. SIMULATION SETUP

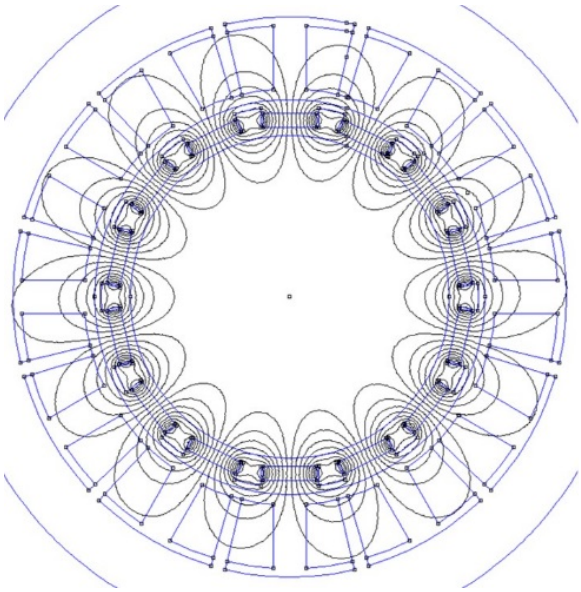

FIGURE 11. PLASTIC CORE SIMULATED MAGNETIC FIELD

are placed at the front and the back of the rotor. they can suspend the rotor while covering the minimum length of the rotor. Each of the short sleeves has a radial component to prevent the rotor from moving front and back, and an axial component to maintain the centeredness of the rotor as shown in Fig. 9. In this way, the short sleeve bearings do not take any space in the air gap between the stator and the rotor. The minimum size of the air gap is thus not bounded by the thickness of the bearing, and the air gap can be made as small as possible for better efficiency of torque generation. Teflon coating can again be applied to the bearings for even lower friction.

SIMULATION

The effectiveness of the motor part of the RIM Propeller is predicted in Finite Element Method Magnetics(FEMM) simulation. A motor is more effective if it can generate more torque given the same current. This motor constant defined as the ratio between the torque output and the current input depends on the number of winding, the size of the stator core, the permeability of the stator core, the strength of the permanent magnet and the size of air gap. To quantify the motor constants, the plastic stator as shown in Fig. 5. and the steel stator as shown in Fig. 7 are modeled and evaluated in a 2D finite element analysis software (FEMM). Only the three different cases (plastic core, 2 different continuous iron cores with thin or thick rings) are simulated because the discontinuous steel core stator was proven not working in preliminary experiments.

The motors are simplified before setting up the FEMM. Since the simulation is in 2D, the motor is assumed to have a constant thickness of 4mm. The actual thickness of the stator core is approximately 3.81mm as it consists of 6 layers of 0.635mm thick laminated steel sheets. With the coil windings, the thickness of the stator becomes approximately 8mm to 10mm. This simulation thickness approximation turned out to be appropriate after comparing the simulation results summarized in Tab. 1 and the Fig. 11 and Fig. 12. The materials, direction of the field generated by permanent magnets and coil winding directions are all setup as shown in Fig. 10. In Fig. 12, the positive winding represents the wire coming out of the page while the negative winding represents the wire going into the page. In all simulations, the air gap and the rotor are kept the same, only the stator geometry and material are changed. Each phase of the coils are simulated to have 0.5A of current. Only the two phases are turned on for the simulation to match the operating conditions of our brushless DC motor(Y connection and square wave signal). The rotor is rotated by a small angular displacement to find the maximum torque the motor can achieve. The simulation was performed with a mesh sizing of 0.1mm inside the stator and automatic mesh sizing outside the stator.

The magnetic field visualization shows that continuous steel core is generating torque more effectively than the plastic core. Comparing the Fig. 11 and Fig. 12, the magnetic field from the magnets are barely influenced by the plastic core. The magnetic field in the steel core is highly concentrated in the cores and the field is circulating between the adjacent poles of the stator, preventing the field from escaping the motor.

The importance of the thickness of the outer ring connecting all the poles are also evaluated. A thicker ring will be able to conduct the magnetic field better, just like a thicker wire has better

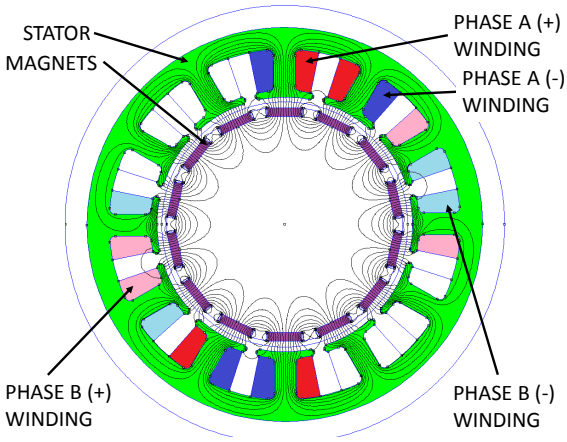

FIGURE 12. STEEL THICK EXTERIOR RING SIMULATED MAGNETIC FIELD

TABLE 1. SIMULATED TORQUE RESULT.

motor Type	Max. Torque(Nm)
Plastic stator	6.558×10^{-4}
Steel stator 0.5mm Ring	3.557×10^{-3}
Steel stator 2mm Ring	3.564×10^{-3}

electrical conductivity. A thicker ring also makes the stator more rigid. Two ring thickness are compared and they are 0.5mm and 2mm. The predicted torque for three cases–the plastic stator, the steel stator with 0.5mm ring (33mm overall diameter) and the steel stator with 2mm ring (36mm overall diameter)–are summarized in Table. 1. The steel stators generate almost 4 times more torque than the plastic stator when they are provided with the same 0.5A current. The thickness of the outer ring is not making a big different in the motor constant at this current setting. It might make a big difference when the current is higher and the overall magnetic field is stronger.

EXPERIMENT

The goal of the experiment is to find how variations in constructing the RIM propeller affects its performance. In three case studies, the thrust outputs of four variations of the micro RIM propellers are evaluated. In each case, only one parameter of the design is changed, and those parameters include the bearing, the stator material and the outer ring thickness. The first case tests the two kinds of proposed bearings(Fig. 8 and Fig. 9) with the same plastic stator. Since the air gap is kept the same (1.5mm, the thickness of the thinnest long sleeve bearing we can

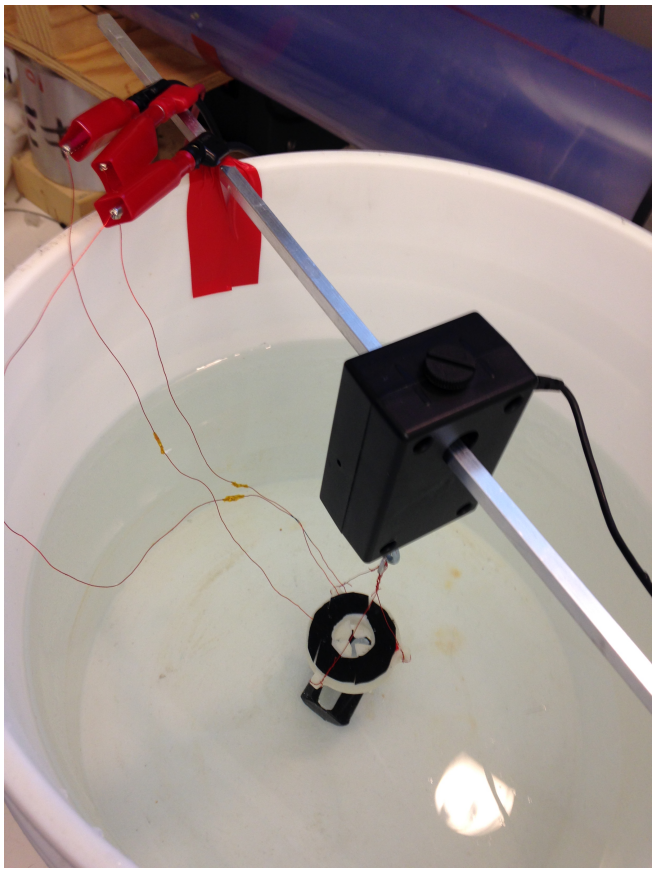

FIGURE 13. THURST MEASUREMENT EXPERIMENT SETUP

3D print), the two bearings are expected to deliver similar performance. The second case compares the thrust outputs from the plastic motor and the continuous steel motor with 0.5mm outer ring. Short sleeve bearings are used for both motors in this case study. The steel motor is expected to produce more thrust while consuming less current. In the third case study, two continuous steel stators, one with 0.5mm outer ring and the other with 2mm outer ring, are compared. Based on the prediction of the simulation, they should produce similar thrust and consume similar amount of current. Short sleeve bearings are also used for both motors in this case study.

The experiment setup is shown in Fig. 13. The overall concept is to hang the RIM propeller on a structure and allow it to propel water upward. The increase in tension force in the hanging structure will be equal to the thrust generated by the RIM propeller. In practice, the RIM propeller was mounted inside a basket hanging down from a dynamometer. The model of dynamometer is called 'Vernier' and it has a sensing range from 0 to 10N. The RIM propeller and the basket were placed inside a bucket of water. The bucket is 30 cm in diameter and 28 cm deep. It was filled with water measuring 17 cm deep. The dy-

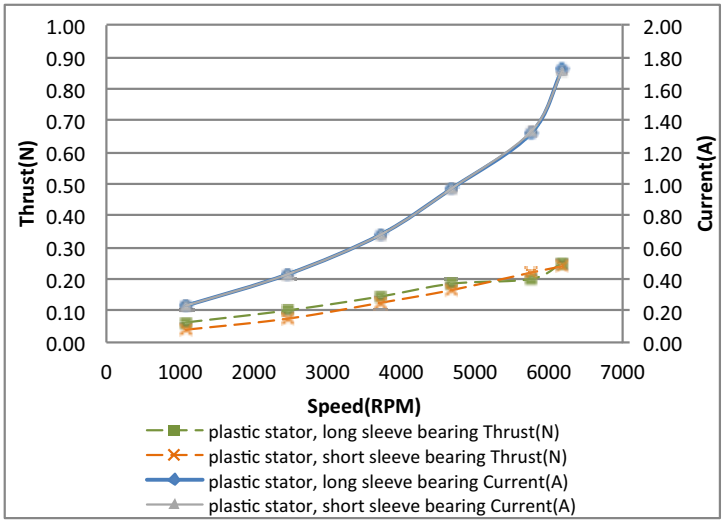

FIGURE 14. THRUST, CURRENT AND SPEED PLOT FOR TWO PLASTIC MOTORS WITH DIFFERENT BEARINGS

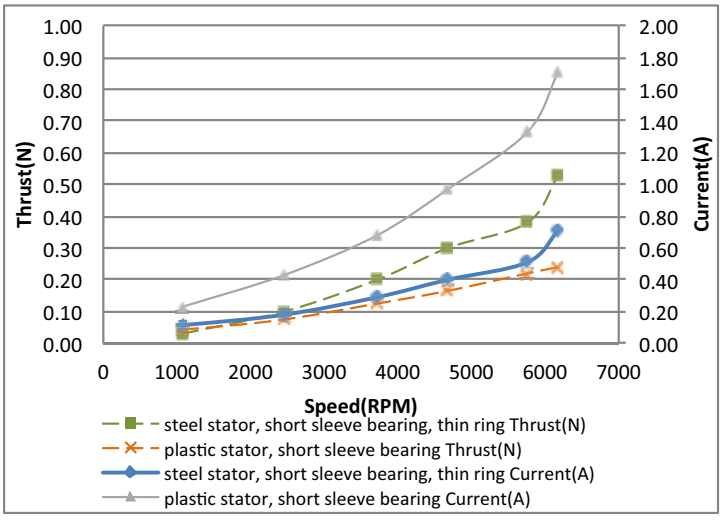

FIGURE 15. THRUST, CURRENT AND SPEED PLOT FOR PLASTIC MOTOR AND STEEL MOTOR

namometer was mounted above the bucket. The propeller was placed 10cm below the water surface, allowing the outgoing flow to dissipate. In order for the propeller to stay at the center of the bucket without moving left and right, a weight of 33.4g was connected to the bottom of the RIM propeller. The weight did not touch the bottom of the bucket. All the cables used in this hanging structure were copper wires, as they were thin and less affected by the water turbulence. The weight of the whole structure was subtracted from the dynamometer reading. The result indicated only the additional pulling force which was equivalent to the thrust. A LabVIEW interface was used to control the speed of the propeller. The voltage input was set to be 10V. A Turnigy 6A electronic speed controller (ESC) was used to create the alternating electrical inputs to the motor. The voltage and current to the motor is monitored. The ESC itself consumed 0.09A at 10V.

In case 1, the RIM propellers with different bearings had almost the same performance. The resulting measurement of current consumption and thrust output are plotted in Fig. 14. At the highest speed which is 6180rpm, both RIM propellers were generating 0.24N to 0.25N of thrust and consuming around $10V \times 1.71A = 17.1W$ of electrical power. The same plastic stator with different bearings consumed almost the same amount of current and produced similar thrust output at all six speeds. The motor with full-length sleeve bearing was producing slightly higher thrust at lower speed compared to the one with short sleeve bearings. In case 2, the RIM propeller with the continuous steel stator produced about twice the thrust and consumed about half the current compared to the one with the plastic stator. The thrust, current and speed plot are shown in Fig. 15. At 6180rpm which is the highest speed the steel motor was producing 0.53N

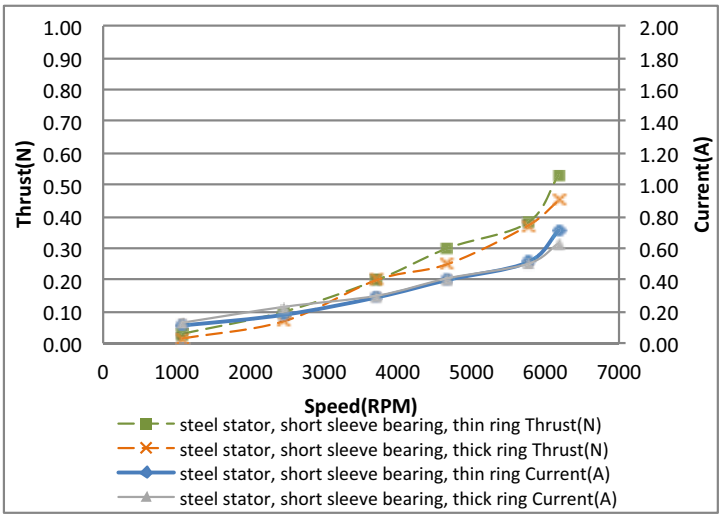

FIGURE 16. THRUST, CURRENT AND SPEED PLOT FOR TWO STEEL MOTORS WITH DIFFERENT RING THICKNESS

of thrust and consumes $10V \times 0.71A = 7.1W$ compared to the 0.24N and 17.1W from the plastic motor. The continuous steel stator was superior in performance and efficiency compared to the plastic stator. In case 3, the RIM propellers with continuous steel stator of different values of their outer ring thickness generated similar performance. The thrust, current and speed plot are shown in Fig. 16. For all speed ranges, the motor with 2mm ring consumes 10 percent more current but generate slightly smaller thrust than the one with 0.5mm ring. This difference was not expected, but it may be attributed to the difference in manufacturing quality.

DISCUSSION

In this section, several of the key observations and understandings of the micro RIM propeller design are presented. First observation is related to the conversion of magnetic energy to mechanical work including the air gap and the stator magnetic field preservation are discussed. They are followed by the comparison of different bearing designs on friction reduction. This particular RIM propeller prototype is also evaluated in comparison to a micro pump, the best propulsion system of similar size. In the end, an integration of the RIM propeller into an AUV is presented.

The air gap between the stator pole and the rotor pole is one of the key parameters that determines the performance of the system. If each magnetic sources are viewed as a coupled north pole and south pole, the force between a rotor pole and a stator pole will follow this equation:

$$F = \frac{\mu_0 q_r q_s}{4\pi x^2} \tag{1}$$

In this equation, the F is the force induced by the magnetic field interaction while μ_0 represents the permeability of free space, q_r and q_s the equivalent charges of magnetic poles on the rotor and stator respectively. The variable x represents the distance between the stator pole and and the closest rotor pole. This distance is the air gap size. Torque is force times length, and it is expected to increase quadratically as the air gap size reduces. The air gap must be made as small as possible for higher torque generation.

The outer ring of the steel stator is necessary but its thickness is not critical. The discrete stator core design in Fig. 6 did not even turn the rotor because it did not have the outer ring to preserve and enhance the magnetic field. The continuous steel stator as shown in Fig. 7 can produce mechanical work output efficiently, while the case study on different outer ring thickness shows that a thicker ring may not necessarily improve the efficiency as indicated in Fig. 16. The ring helps circulating and preserving the magnetic field generated by the coils. In a RIM propeller or any other low power systems, it can be thin and it still guarantees the performance. However, in terms of manufacturability and rigidity, a slightly thicker outer ring is preferred. From the simulation results in Table 1 the increase of thickness is 4 times but the increase in the torque is minor. Additionally, each layer of the lamination in the stator with 0.5mm ring was easy to deform during the winding or assembling process. The flexing of the stator would cause the rotor to rub against the stator and wear out quickly. In contrast, those with 2mm ring are less subjective to any possible deformation during the coil winding process and provide more consistent performance.

Two different kinds of bearings for this micro RIM propeller are all viable solutions. Both bearings support and maintain the rotor in the center. The long sleeve bearing uses low friction contact surface coated by Teflon while the short sleeve bearing supports the rotor from two edges with a minimum contact surface area. In terms of the performance, they are close to each other. The experiment results show that they yield almost the same thrust given the similar power input. Waterproof sealing is achieved differently on systems with different bearings. Systems with long sleeve bearings enclose the stators in the waterproof housing. While systems with short sleeve bearings cannot enclose the stator, the whole stator can be covered in epoxy so it is waterproof on its own. One of the possible advantages of short sleeve bearing over long sleeve bearing is on the highest obtainable motor efficiency. To improve motor efficiency it is essential to reduce the air gap between the stator and the rotor. The minimum gap size for RIM propellers with long sleeve bearing is bounded on the thickness of the bearing. In systems with short sleeve bearings, the air gap can be made as small as possible.

TABLE 2. SIZE AND THRUST COMPARISON OF RIM PROPELLER AND MICRO PUMPS.

Actuator	Micro Pump	Micro RIM Propeller
Size	$40 \times 26 \times 25mm$	$\o 33 \times 12mm$
Power Consumption	$7.1W$	$7.1W$
Highest Possible Thrust	$0.25N$	$0.4N$
Volume Ratio	100%	40%
Thrust Ratio	100%	160%

This RIM propeller generates more thrust than other internal propulsion systems of a similar size and power requirement. The specific comparison here in Table 2 is between this RIM propeller and TCS M400S micro pump, the best solution found at this size scale. At 40% volume, this RIM propeller generates 160% thrust compared to the best micro pump. With further improvement on the quality of manufacturing and propeller blade analysis, RIM propeller can become one of the best options for powerful micro AUVs.

RIM propellers can be easily integrated into micro AUVs. They work similarly to regular propellers; they can be placed behind the hull of the vehicle, mounted on the surface of the vehicle, or built into the robot as ducted propellers. In the robot shown in Fig. 3, RIM propellers are placed inside the ducts in the robot. A robot of this size and thrust requirement is almost impossible to be built with either micro pumps or regular ducted propellers. With the compact RIM propeller, the researchers can put two of them in the robot, one in each duct. They are ex-

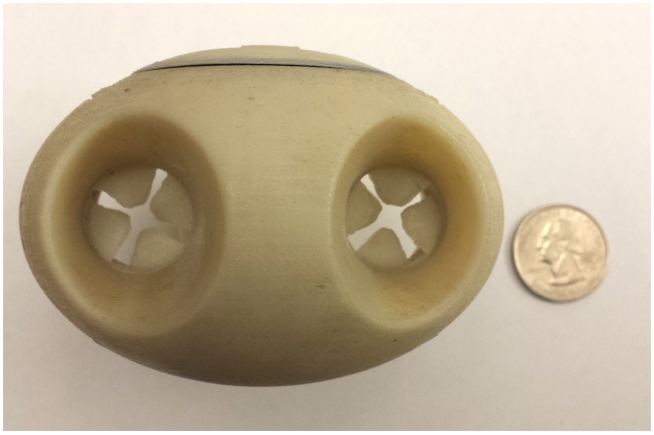

FIGURE 17. THE ROBOT WITH RIM PROPELLERS INSIDE

pected to produce more than 0.8N thrust to allow the robot to transverse in the pipe freely. By differentiating the thrust from each propeller, the vehicle can turn at various radius of curvature. In addition, all these performances can be achieved with a pair of 7.4V 350mAh Lipo batteries, and it is expected to run at maximum speed for 20 minutes. Videos of the RIM propeller working and the robot working can be found on our website at http://mechatronics.mit.edu/development-of-micro-auvs-for-pipe-inspection/.

CONCLUSION

In this paper, we presented the design, manufacturing and performance analysis of a micro RIM propeller. This RIM propeller has no shaft, and is supported by relatively simple bearing systems. A few variations of the RIM propeller, including that of different stator materials, stator sizes and bearing structures are compared and discussed. The best micro RIM propeller prototype is 33mm in diameter, 12mm in depth and 16g in weight, and it is capable of producing 0.4N thrust in static water given 7.1W power input. As an assembly the micro RIM propeller is watertight and easy to be integrated into micro AUVs. RIM propellers can be one of the best actuation systems for fast and highly maneuverable micro AUVs for applications in pipes, power plant interior and many other confined or open environments.

ACKNOWLEDGEMENT

The financial support from MIT Kuwait Center during the course of this work is greatly appreciated. Thanks also go Lei Zhou for advises on brushless DC motor design and David D'Achiardi for his help during the experimentation.

REFERENCES

[1] D. Chatzigeorgiou, R. Ben-Mansour, A. K., and Youcef-Toumi, K., 2012. "Design and evaluation of an in-pipe leak detection sensing technique based on force transduction". In ASME International Mechanical Engineering Congress and Exposition.

[2] D. Chatzigeorgiou, K. Youcef-Toumi, A. K., and Ben-Mansour, R., 2011. "Analysis and design of an in-pipe system for water leak detection". In ASME International Design Engineering Technical Conferences and Design Automation Conference.

[3] D. Chatzigeorgiou, K. Y.-T., and Ben-Mansour, R., 2014. "Design of a novel in-pipe reliable leak detector". *IEEE/ASME Transactions on Mechatronics*.

[4] Chatzigeorgiou D., Y.-T. K., and R., B.-M., 2014. "Modeling and analysis of an in-pipe robotic leak detector". In IEEE International Conference on Robotics and Automation.

[5] Chatzigeorgiou D., Wu You, Y.-T. K., and R., B.-M., 2013. "Reliable sensing of leaks in pipelines". In ASME Dynamic Systems and Control Conference.

[6] Mazumdar, A., Fittery, A., Ubellacker, W., and Asada, H., 2013. "A ball-shaped underwater robot for direct inspection of nuclear reactors and other water-filled infrastructure". In Robotics and Automation (ICRA), 2013 IEEE International Conference on, pp. 3415–3422.

[7] Koji, K., 1999. "Underwater inspection robot: Airis-21". *Nuclear Eng. Design,* ***188***, pp. 327–335.

[8] B. Cho, S. Byun, C. S., and etc, 2004. "Keprovt: Underwater robotic system for visual inspection of nuclear reactor internals". *Nuclear Eng. Design,* ***231***, pp. 327–335.

[9] y Alvarado, P. V., and Youcef-Toumi, K., 2006. "Design of machines with compliant bodies for biomimetic locomotion in liquid environments". *ASME Journal of Dynamic Systems measurement and Control*.

[10] Cloitre, A., Subramaniam, V., Patrikalakis, N., and Valdivia y Alvarado, P., 2012. "Design and control of a field deployable batoid robot". In Biomedical Robotics and Biomechatronics (BioRob), 2012 4th IEEE RAS EMBS International Conference on, pp. 707–712.

[11] Mazumdar, A., 2013. "Control configured design for smooth, high-maneuverable, underwater vehicles". PhD thesis, Massachusetts Institute of Technology.

[12] Edwards, I., 1988. Eletric motor rotor comprising a propeller. British Patent Application GB 2 200 802 A.

[13] S.M. Abu Sharkh, S. L., and Turnock, S., 2004. "Structurally integrated brushless pm motor for miniature propeller thrusters". In IEEE Proc. Electr. Power Appl., Vol. 151.

[14] Holt, J., and Kennedy, G., 1994. Propulsion system for submarine vessels. US Patent 5306183.